J Mol Model (2014) 20:2458
DOI 10.1007/s00894-014-2458-3

ORIGINAL PAPER

Interplay between halogen and chalcogen bonding in the XCl···OCS···NH_3 (X = F, OH, NC, CN, and FCC) complex

Qiang Zhao

Received: 30 June 2014 / Accepted: 1 September 2014 / Published online: 20 September 2014

Abstract The interplay between halogen and chalcogen bonding in the XCl OCS and XCl OCS NH_3 (X = F, OH, NC, CN, and FCC) complex was studied at the MP2/6-311++G(d,p) computational level. Cooperative effect is observed when halogen and chalcogen bonding coexist in the same complex. The effect is studied by means of binding distance, interaction energy, and cooperative energy. Molecular electrostatic potential calculation reveals the electrostatic nature of the interactions. Cooperative effect is explained by the difference of the electron density. Second-order stabilization energy was calculated to study the orbital interaction in the complex. Atoms in molecules analysis was performed to analyze the enhancement of the electron density in the bond critical point.

Keywords Chalcogen bonding · Cooperativity · Halogen bonding · Interplay · Molecular electrostatic potential

Introduction

Noncovalent interactions play a prominent role in crystal engineering, biological recognition, and reaction selectivity [1–3]. Among them, halogen bonding has attracted considerable attention in recent years [4]. A great many of experimental and theoretical investigations have been made to enclose the important applications of halogen bond [5–14]. Politzer et al. explained halogen bond by using the σ−hole concept: Halogen bond is driven by the electrostatic interaction between the σ−hole of the halogen atom and a negative site [15–23]. Noncovalent interactions between covalently bonded atoms of group VI and Lewis bases are also σ−hole interactions, which are commonly called chalcogen bond [24–28]. For example, S S and S π interactions can stabilize folded protein structures and play important roles in crystal engineering [25–27].

The cooperativity between two or more noncovalent interactions has received great attention. Interplay between halogen bonding and other intermolecular interactions have been proved to be essential in supramolecular architectures and biological design [29–36]. For example, there exist synergetic effects between halogen bonding and hydrogen bonding [37–39], pnicongen bonding [40], cation–π interaction [41], anion–π interaction [42], and π–π stacking [43]. The strength of the noncovalent interaction can be enhanced through cooperativity.

Recently, Manna et al. investigated the regioselective deiodination of thyroxine by iodothyronine deiodinase mimics [44]. They found an unusual mechanistic pathway involving cooperative chalcogen and halogen bonding. Their experimental and theoretical investigations reveal that the interaction between the iodine and chalcogen and the peri-interaction between two chalcogen atoms are important for the deiodinase activity. Metrangolo [45] studied the behavior of di-selenol enzyme mimics and found that the interplay between halogen and chalcogen bonding played an important role in the activation of thyroid hormones. These research works indicate that there exists cooperativity between halogen and chalcogen bonding.

In this paper, the XCl OCS and XCl OCS NH_3 (X = F, OH, NC, CN, and FCC) complex was designed to study the interplay between halogen and chalcogen bonding. These complexes contain Cl O halogen bonding and S N chalcogen bonding. Quantum chemical calculations were performed to study how these two noncovalent interactions interplay in the complexes.

Q. Zhao (✉)
Department of Chemical Engineering, Zibo Vocational Institute, Zibo 255314, Shandong Province, People's Republic of China
e-mail: qzhaochem02@gmail.com

Computational details

The geometries of the monomers and complexes were optimized at the MP2/6-311++G(d,p) computational level. All of the optimized structures were characterized as minima in the potential energy surface by verifying that all the vibrational frequencies are real. The basis set superposition error (BSSE) was eliminated by using the standard counterpoise correction (CP) method of Boys and Bernardi [46]. All calculations were carried out with the Gaussian 09 suite of programs [47]. The density difference in complex formation was analyzed by evaluating the difference between the total electron densities of the XCl OCS NH_3 complex and individual moieties (XCl, OCS, and NH_3), which was fulfilled by the Multiwfn programs [48]. Natural bond orbital (NBO) analysis [49] was performed by using the NBO program implemented in Gaussian 09. The atoms in molecules (AIM) analysis [50] was performed with the help of AIMAll [51] using the MP2 wavefunctions.

The interaction energy of the halogen and chalcogen bonding in the dimer was calculated using Eqs. 1 and 2, respectively.

$$\Delta E_{\mathrm{hal}} = E_{\mathrm{XC1}\cdots\mathrm{OCS}} - (E_{\mathrm{XCI}} + E_{\mathrm{OCS}}) \quad (1)$$

$$\Delta E_{\mathrm{chal}} = E_{\mathrm{OCS}\cdots\mathrm{NH3}} - (E_{\mathrm{OCS}} + E_{\mathrm{NH3}}) \quad (2)$$

The interaction energy of the halogen and chalcogen bonding in the trimer was given by Eqs. 3 and 4, respectively.

$$\Delta E'_{\mathrm{hal}} = E_{\mathrm{tirmer}} - E_{\mathrm{XC1}} - E_{\mathrm{OCS}\cdots\ \mathrm{NH3}} - \Delta E_{\mathrm{XC1-NH3}} \quad (3)$$

$$\Delta E'_{\mathrm{chal}} = E_{\mathrm{trimer}} - E_{\mathrm{XC1}\cdots\ \mathrm{OCS}} - E_{\mathrm{NH3}} - \Delta E_{\mathrm{XC1-NH3}} \quad (4)$$

Where $\Delta E_{\mathrm{XCl-NH3}}$ is the interaction energy of molecules XCl and NH_3 in the geometry they adopt in the trimer.

The total interaction energy and the cooperative energy in the trimer were calculated using Eqs. 5 and 6, respectively.

$$\Delta E_{\mathrm{total}} = E_{\mathrm{trimer}} - (E_{\mathrm{XC1}} + E_{\mathrm{OCS}} + E_{\ \mathrm{NH3}}) \quad (5)$$

$$E_{\mathrm{coop}} = \Delta E_{\mathrm{total}} - \Delta E_{\mathrm{hal}} - \Delta E_{\mathrm{chal}} - \Delta E_{\mathrm{XC1-NH3}} \quad (6)$$

Results and discussion

The halogen- and chalcogen-bonded dimers are optimized at the MP2/6-311++G(d,p) level. For the halogen bonding, the Cl O distance varies from 2.797 Å in the FCl OCS complex to 3.057 Å in the FCCCl···OCS complex. The increasing order of the Cl···O distance is FCl···OCS<CNCl···OCS< HOCl···OCS<NCCl···OCS<FCCCl···OCS. The S···N distance in the OCS···NH_3 complex is 3.290 Å, which is larger than that in the halogen-bonded complex.

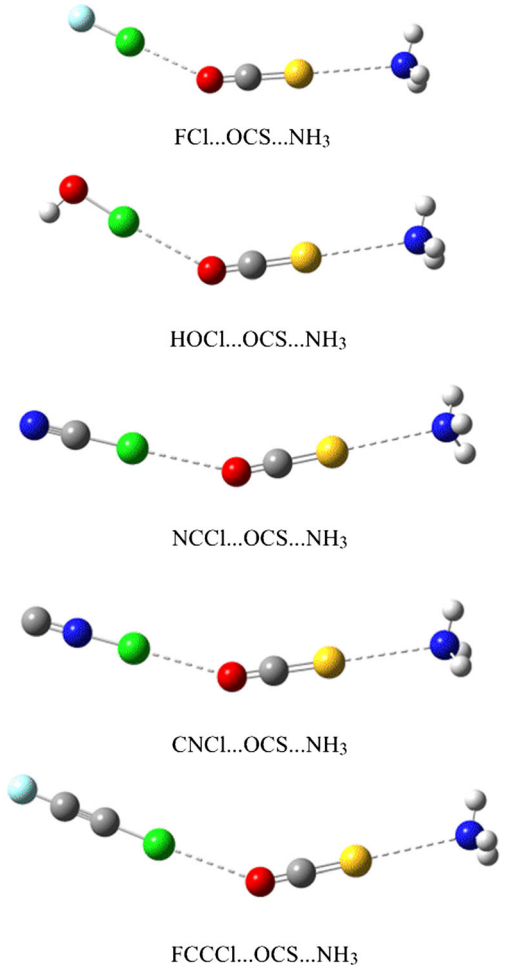

Fig. 1 Optimized structures of the XCl···OCS···NH_3 (X = F, OH, NC, CN, and FCC) complex

The optimized structures of the XCl···OCS···NH_3 (X = F, OH, NC, CN, and FCC) trimer are shown in Fig. 1. The binding distance of the timer and the variation of the binding distance are summarized in Table 1. The binding distance in the trimer has been shortened with respect to the dimer. The decrement of the Cl···O distance is in the range of 0.025 −0.064 Å, while the shortening of the S···N distance varies

Table 1 Binding distance (in Å) and the variation of the binding distance in the XCl···OCS···NH_3 (X = F, HO, NC, CN, and FCC) complex calculated at the MP2/6-311++G(d,p) level

Complex	$R_{\mathrm{Cl\ O}}$	$\Delta R_{\mathrm{Cl\ O}}$	$R_{\mathrm{S\ N}}$	$\Delta R_{\mathrm{S\ N}}$
FCl···OCS···NH_3	2.759	−0.038	3.257	−0.033
HOCl···OCS···NH_3	2.907	−0.030	3.275	−0.015
NCCl···OCS···NH_3	2.974	−0.064	3.262	−0.028
CNCl···OCS···NH_3	2.852	−0.037	3.254	−0.036
FCCCl···OCS···NH_3	3.032	−0.025	3.276	−0.014

Table 2 Variations of the X−Cl bond length (in Å) and the frequency shift of X−Cl stretching vibration (in cm^{-1}) at the MP2/6-311++G(d,p) level

Complex	ΔR_{X-Cl}	Δv_{X-Cl}
FCl···OCS	0.005	−8.84
HOCl···OCS	0.004	−5.94
NCCl···OCS	0.001	−1.57
CNCl···OCS	0.003	−6.02
FCCCl···OCS	0.001	−0.66
FCl···OCS···NH_3	0.006	−11.34
HOCl···OCS···NH_3	0.005	−7.39
NCCl···OCS···NH_3	0.002	−1.87
CNCl···OCS···NH_3	0.004	−7.50
FCCCl···OCS···NH_3	0.002	−1.08

from 0.014 to 0.036 Å. This result shows that there exists interplay between halogen and chalcogen bonding. One can see that the decrement amount of the Cl···O distance is larger than that of the S···N distance, indicating that the influence on halogen bonding is more prominent than chalcogen bonding. The $R_{Cl\cdots O}$ value is decreased in the order of NCCl···OCS···NH_3 > FCl···OCS···NH_3 > CNCl···OCS···NH_3 > HOCl···OCS···NH_3 > FCCCl···OCS···NH_3, whereas the shortening of the S···N distance is increased in the order: FCCCl···OCS···NH_3 < HOCl···OCS···NH_3 < NCCl···OCS···NH_3 < FCl···OCS···NH_3 < CNCl···OCS···NH_3. This order is almost the same except for NCCl···OCS···NH_3 and CNCl···OCS···NH_3, which indicates that the variation of the binding distance of the halogen and chalcogen bonding presents a similar tendency.

Table 2 presents the variations of the X−Cl bond length and the frequency shift of X−Cl stretching vibrations in the studied complexes. One can see that the X−Cl bond is elongated in the XCl···OCS and XCl···OCS···NH_3 complexes. Accompanied with the formation of the complex, the X−Cl stretching vibration shows a red shift. For the XCl···OCS complex, the ΔR_{X-Cl} value decreases in the order FCl > HOCl > CNCl > NCCl = FCCCl, which is not the same as binding distance. The bond elongation is larger in the XCl···OCS···NH_3 complex than that in the XCl···OCS complex. The frequency shift becomes more negative in the trimer than that in the dimer, which is consistent with the bond elongation.

The interaction energy for the halogen-bonded dimer ranges from −1.326 kcal mol^{-1} in the CNCl···OCS complex to −0.53 kcal mol^{-1} in the HOCl···OCS complex. The interaction in the OCS···NH_3 complex is −0.909 kcal mol^{-1}, which is less negative than that in the FCl···OCS, NCCl···OCS, and CNCl···OCS complexes. Table 3 presents total interaction energy in the XCl···OCS···NH_3 complex, the interaction energy of the halogen and chalcogen bonding interactions in the trimer, and the variation of the interaction energy compared to the dimer. One can see that $\Delta\Delta E_{hal}$ and $\Delta\Delta E_{chal}$ values are negative, indicating that halogen and chalcogen bonding are both strengthened in the trimer. This is consistent with the shortening of the binding distance. The $\Delta\Delta E_{chal}$ value is more negative than that of $\Delta\Delta E_{hal}$, which implies that chalcogen bonding gains more stability than halogen bonding. This is not in accord with the variation of the binding distance, which has been verified in the study of cooperative halogen and pnicogen bonding [40]. For halogen bonding, the increment of the interaction energy varies in the order: HOCl···OCS···NH_3 < FCCCl···OCS···NH_3 < NCCl···OCS···NH_3 < FCl···OCS···NH_3 < CNCl···OCS···NH_3. This sequence is the same as the interaction energy of the halogen-bonded dimer. A similar order is found for the chalcogen bond, except for an inverse sequence of FCl···OCS···NH_3 and CNCl···OCS···NH_3. The increased percentage for the interaction energy of the halogen bonding is almost the same (15 ~18 %), and it is 12 ~26 % for the chalcogen bonding. In the HOCl···OCS···NH_3 and FCCCl···OCS···NH_3 complexes, the increased percentage for the interaction energy of the halogen bonding is smaller than that of the chalcogen bonding, which is attributed to the relative bonding strength. The calculations are consistent with the conclusion that the stronger noncovalent interaction has a bigger effect on the weaker one [39].

In order to evaluate the synergetic effects between halogen and chalcogen bonding, the cooperative energy (E_{coop}) of the trimer was calculated using Eq. 6, which is also listed in Table 3. One can see that all the cooperative energies are

Table 3 Total interaction energy (ΔE_{total}) in the XCl···OCS···NH_3 complex, the interaction energy of the halogen bonding (ΔE_{hal}) and chalcogen bonding (ΔE_{chal}) in the trimer, and the variation of the interaction energy compared to the dimer ($\Delta\Delta E_{hal}$ and $\Delta\Delta E_{chal}$) at the MP2/6-311++G(d,p) level

Complex	ΔE_{total}	ΔE_{hal}	$\Delta\Delta E_{hal}$	ΔE_{chal}	$\Delta\Delta E_{chal}$	E_{coop}
FCl···OCS···NH_3	−2.422	−1.390	−0.202	−1.146	−0.237	−0.325
HOCl···OCS···NH_3	−1.543	−0.625	−0.095	−1.022	−0.113	−0.104
NCCl···OCS···NH_3	−2.196	−1.137	−0.160	−1.080	−0.171	−0.310
CNCl···OCS···NH_3	−2.612	−1.538	−0.212	−1.139	−0.230	−0.377
FCCCl···OCS···NH_3	−1.655	−0.710	−0.099	−1.035	−0.126	−0.135

Table 4 $V_{S,max}$(Cl) (in kcal mol^{-1}) in the XCl (X = F, OH, NC, CN, and FCC) molecule and $V_{S,max}$(S) in the XCl···OCS complex calculated at the MP2/6-311++G(d,p) level

Molecule	$V_{S,max}$(Cl)	complex	$V_{S,max}$(S)
FCl	44.1	FCl···OCS	23.1
HOCl	26.4	HOCl···OCS	19.1
NCCl	36.9	NCCl···OCS	22.9
CNCl	44.7	CNCl···OCS	23.6
FCCCl	23.4	FCCCl···OCS	19.5

negative, which indicates that halogen and chalcogen bonding work in concert with each other and enhance each other's strength in the XCl···OCS···NH_3 (X = F, OH, NC, CN, and FCC) complex. The E_{coop} value becomes more negative in the order: HOCl···OCS···NH_3 < FCCCl···OCS···NH_3 < NCCl···OCS···NH_3 < FCl···OCS···NH_3 < CNCl···OCS···NH_3. This sequence is the same as the interaction energy of the halogen-bonded dimer. This implies that stronger halogen bonding makes the interplay between halogen and chalcogen bonding interactions more intensive.

Politzer et al. have pointed out that σ−hole interaction including halogen and chalcogen bonding is electrostatically driven. They found that molecular electrostatic potential (MEP) V(r) was very useful for interpreting noncovalent interactions. V(r) on a molecule surface is designated V_S(r) and the donating and accepting tendencies of halogen and chalcogen bonding can be related quantitatively to most positive values, $V_{S,max}$ and most negative values, $V_{S,min}$. The $V_{S,max}$ and $V_{S,min}$ values in the relevant atoms at the 0.001 electrons per Bohr^{-3} isodensity surfaces were calculated at the MP2/6-311++G(d,p) level. The results are summarized in Table 4. The $V_{S,max}$ value in XCl (X = F, OH, NC, CN, and FCC) increases in the order: FCCCl<HOCl<NCCl<FCl<CNCl. Except FCCCl and HOCl, this sequence is consistent with the stability of the XCl···OCS complex. For halogen bonding, the O atom in the OCS molecule is halogen bond donor. The

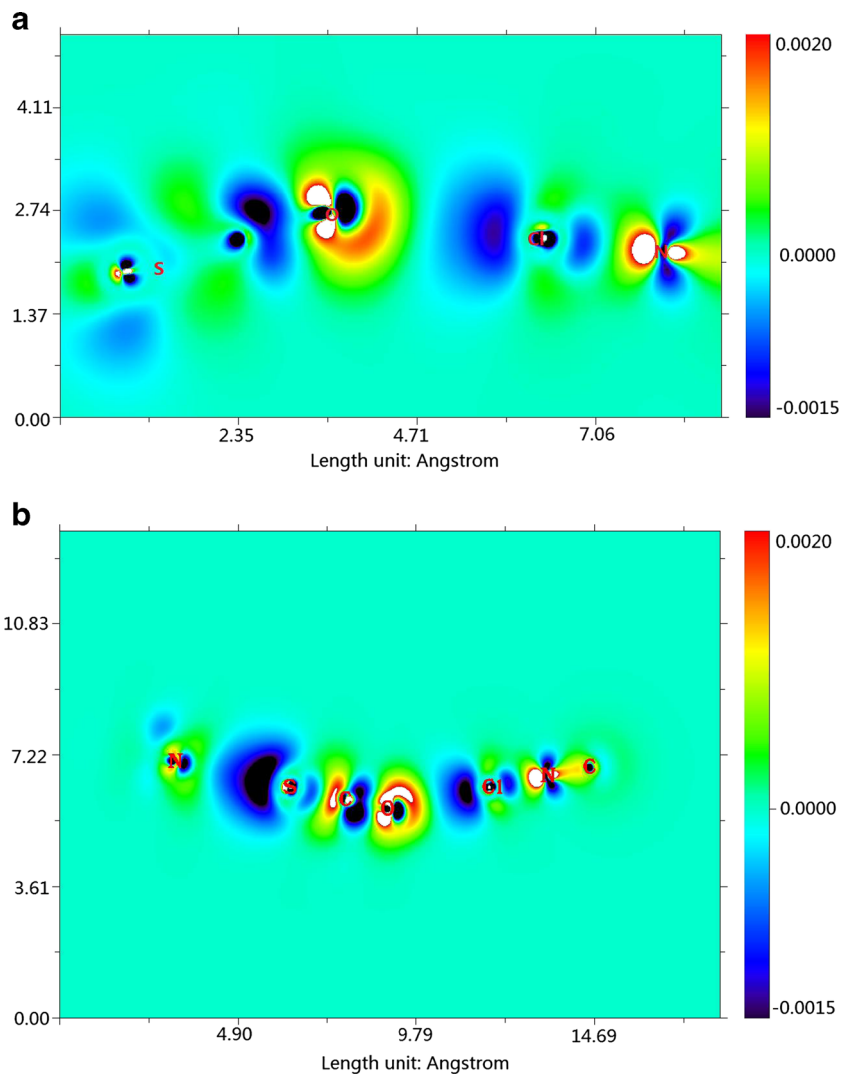

Fig. 2 Computed density difference color-filled map for the CNCl···OCS and CNCl···OCS···NH_3 complexes

Table 5 Second-order stabilization energies (E^2, in kcal mol^{-1}) in the XCl···OCS and XCl···OCS···NH_3 (X = F, OH, NC, CN, and FCC) complexes

Complex	$E^2_{LP(O)\rightarrow\sigma^*(X-Cl)}$	Complex	$E^2_{LP(O)\rightarrow\sigma^*(X-Cl)}$	$E^2_{LP(N)\rightarrow\sigma^*(C-S)}$
FCl···OCS	2.40	FCl···OCS···NH_3	2.76	2.10
HOCl···OCS	1.31	HOCl···OCS···NH_3	1.52	2.01
NCCl···OCS	0.70	NCCl···OCS···NH_3	0.81	2.08
CNCl···OCS	1.54	CNCl···OCS···NH_3	1.81	2.11
FCCCl···OCS	0.60	FCCCl···OCS···NH_3	0.70	2.00

$V_{S,min}$ value of the O atom in the OCS molecule is −13.2 kcal mol^{-1}, whereas it is −18.7 kcal mol^{-1} in the OCS···NH_3 complex. That is to say the electron donating ability of the O atom in the OCS···NH_3 complex strengthened, which contributes to the enhancement of the halogen bonding in the trimer. For chalcogen bonding, the S atom is electron acceptor. The positive potential on the sulfur of the O=C=S molecule is a positive region on a noncovalent group VI atom in contrast to many that are along the extensions of the two bonds in divalent sulfur-containing molecules [14]. The $V_{S,max}$ value of the S atom in the OCS molecule is 17.8 kcal mol^{-1}, and this value increases in the XCl···OCS complex. The $V_{S,max}$(S) value in the XCl···OCS complex increases in the order: HOCl···OCS<FCCCl···OCS<NCCl···OCS< FCl···OCS<CNCl···OCS. This sequence is the same as the interaction energy of the chalcogen bonding in the trimer. The results show that the interplay between halogen and chalogen bonding does not change the nature of the interaction, which is electrostatic interaction.

Cooperativity between different noncovalent interactions can be explained by polarization, which has been discussed by Politzer et al. [19, 21]. A detailed picture of polarization can be obtained by investigating the difference of the electron density of the complex and the sum of electron densities of the free molecules. Figure 2 shows the computed density difference color-filled map for the CNCl···OCS and CNCl···OCS···NH_3 complexes. One can see from Fig. 2a that the electric field of the lone pair of the O atom causes a decrease of electron density of the Cl atom, and the electron density of the O atom increases due to a rearrangement of electronic charge. From Fig. 2b, the electric field of the lone pair of the O atom causes a stronger decrement of electron density of the Cl atom, indicating the electric field of the lone pair of the O atom becomes more intensive in the CNCl···OCS···NH_3 complex. The region between the S and N atom is similar to that between O and Cl, indicating noncovalent interaction exists. That is to say, inclusion of chalcogen bonding makes the electric field of the lone pair of the O atom more polarized, which contributes to the enhancement of halogen bonding.

To deepen the understanding of the interplay between halogen and chalcogen bonding in the XCl···OCS···NH_3 complex, NBO analysis was performed using the HF/6-311++ G(d,p) density. Halogen bonding can be described as orbital interaction between filled and empty natural bond orbitals. Table 5 lists the second-order stabilization energies (E^2) in the XCl···OCS and XCl···OCS···NH_3 (X = F, OH, NC, CN, and FCC) complexes. For the halogen-bonded dimer, there exists orbital interaction between LP(O) and σ*(X−Cl), whereas LP(N)→σ*(C−S) interaction is in the chalcogen bonding. One can see that $E^2_{LP(O)\rightarrow\sigma^*(X-Cl)}$ is larger in the XCl···OCS···NH_3 complex than that in the XCl···OCS complex, indicating that the orbital interaction of halogen bonding is strengthened in the trimer. $E^2_{LP(N)\rightarrow\sigma^*(C-S)}$ in the OCS···NH_3 complex is 1.93 kcal mol^{-1}, and it increases in the XCl···OCS···NH_3 complex, which implies that the orbital interaction of chalcogen bonding is also enhanced in the trimer. This is consistent with the results of interaction energy and molecular electrostatic potential.

AIM theory is based on a topological analysis of the electron charge density and its Laplacian, which has been successfully applied in characterizing hydrogen bonds and halogen bonds of different strengths in a wide variety of molecular complexes. With this in mind, a topological analysis was performed to gain more insights into the XCl···OCS and XCl···OCS···NH_3 complexes. Table 6 collects the electron density (ρ) at the Cl···O and S···N bond critical points (BCPs). It can be seen that $\rho_{Cl\cdots O}$ in the XCl···OCS···NH_3 complex is larger than that in the XCl···OCS complex. $\rho_{S\cdots N}$ at the S···N bond critical point in the OCS···NH_3 complex is 0.0086 a.u., and it also becomes larger in the trimer. The result of AIM

Table 6 Electron density (ρ, in a.u.) at the Cl···O and S···N bond critical points in the XCl···OCS and XCl···OCS···NH_3 (X = F, OH, NC, CN, and FCC) complexes calculated at the MP2/6-311++G(d,p) level

Complex	$\rho_{Cl\ O}$	Complex	$\rho_{Cl\ O}$	$\rho_{S\ N}$
FCl···OCS	0.0118	FCl···OCS···NH_3	0.0129	0.0092
HOCl···OCS	0.0093	HOCl···OCS···NH_3	0.0099	0.0089
NCCl···OCS	0.0073	NCCl···OCS···NH_3	0.0087	0.0091
CNCl···OCS	0.0098	CNCl···OCS···NH_3	0.0107	0.0092
FCCCl···OCS	0.0059	FCCCl···OCS···NH_3	0.0061	0.0087

analysis is in accord with the geometric and energetic features of the complexes.

Conclusions

In summary, the cooperativity between halogen and chalcogen bonding in the XCl···OCS and XCl···OCS···NH_3 (X = F, OH, NC, CN, and FCC) complexes was studied using quantum chemical calculations. Two types of noncovalent interactions become more stabilized in the trimer. The Cl···O and S···N distance shortened and the interaction energies of halogen and chalcogen bonding become more negative in the trimer. The cooperative energy is negative and stronger halogen bonding makes the interplay between halogen and chalcogen bonding more intensive. Analysis of molecule electrostatic potential, electron density difference, second-order stabilization energy, and electron density at bond critical point gives similar results.

Acknowledgments The author is grateful for the help of the high performance computing center in Shandong University and reasonable advice of Prof. Feng in Shandong University.

References

1. Chalasinski G, Szczesniak MM (2000) Chem Rev 100:4227–4252
2. Rudkevich DM (2004) Angew Chem Int Ed 43:558–571
3. Saalfrank RW, Maid H, Scheurer A (2008) Angew Chem Int Ed 47: 8794–8824
4. Metrangolo P, Resnati G (eds) (2007) Halogen bonding: fundamentals and applications, structure and bonding. Springer, Berlin
5. Corradi E, Meille SV, Messina MT, Metrangolo P, Resnati G (2000) Angew Chem Int Ed 39:1782–1786
6. Metrangolo P, Meyer F, Pilati T, Resnati G, Terraneo G (2008) Angew Chem Int Ed 47:6114–6127
7. Legon AC (2010) Phys Chem Chem Phys 12:7736–7747
8. Metrangolo P, Neukirch H, Pilati T, Resnati G (2005) Acc Chem Res 38:386–395
9. Cavallo G, Metrangolo P, Pilati T, Resnati G, Sansotera M, Terraneo G (2010) Chem Soc Rev 39:3772–3783
10. Auffinger P, Hays FA, Westhof E, Ho PS (2004) Proc Natl Acad Sci U S A 101:16789–16794
11. Parisini E, Metrangolo P, Pilati T, Resnati G, Terraneo G (2011) Chem Soc Rev 40:2267–2278
12. Lu YX, Shi T, Wang Y, Yang HY, Yan XH, Luo XM, Jiang HL, Zhu WL (2009) J Med Chem 52:2854–2862
13. Lu YX, Wang Y, Zhu WL (2010) Phys Chem Chem Phys 12:4543–4551
14. Wang WZ, Tian AM, Wong NB (2005) J Phys Chem A 109:8035–8040
15. Politzer P, Murray JS (2002) Theor Chem Acc 108:134–142
16. Clark T, Hennemann M, Murray JS, Politzer P (2007) J Mol Model 13:291–296
17. Politzer P, Lane P, Concha MC, Ma YG, Murray JS (2007) J Mol Model 13:305–311
18. Politzer P, Murray JS, Clark T (2010) Phys Chem Chem Phys 12: 7748–7757
19. Politzer P, Riley KE, Bulat FA, Murray JS (2012) Comput Theor Chem 998:2–8
20. Politzer P, Murray JS (2013) Chem Phys Chem 17:278–294
21. Politzer P, Murray JS, Clark T (2013) Phys Chem Chem Phys 15: 11178–11189
22. Politzer P, Murray JS (2013) Cryst Eng Comm 15:3145–3150
23. Politzer P, Murray JS (2002) Theor Chem Acc 108:134–142
24. Wang WZ, Ji BM, Zhang Y (2009) J Phys Chem A 113: 8132–8135
25. Iwaoka M, Takemoto S, Tomoda S (2002) J Am Chem Soc 124: 10613–10620
26. Bleiholder C, Werz DB, Köppel H, Gleiter R (2006) J Am Chem Soc 128:2666–2674
27. Bleiholder C, Gleiter R, Werz DB, Köppel H (2007) Inorg Chem 46: 2249–2260
28. Murray JS, Lane P, Politzer P (2008) Int J Quantum Chem 108:2770–2781
29. Vijay D, Sastry GN (2010) Chem Phys Lett 485:235–242
30. Parra RD, Ohlssen J (2008) J Phys Chem A 112:3492–3498
31. Egi M, Sarkhel S (2007) Acc Chem Res 40:197–205
32. Alkorta I, Blanco F, Elguero J (2008) J Phys Chem A 112: 6753–6759
33. Politzer P, Murray JS, Concha MC (2007) J Mol Model 13: 643–650
34. Alkorta I, Blanco F, Elguero J, Estarellas C, Frontera A, Quinonero D, Deya PM (2009) J Chem Theory Comput 5: 1186–1194
35. Frontera A, Quinonero D, Costa A, Ballester P, Deya PM (2007) New J Chem 31:556–560
36. Estarellas C, Frontera A, Quinonero D, Alkorta I, Deya PM, Elguero J (2009) J Phys Chem A 113:3266–3273
37. Lankau T, Wu YC, Zou JW, Yu CH (2008) J Theor Comput Chem 7: 13–35
38. Politzer P, Murray JS, Lane P (2007) Int J Quantum Chem 107:3046–3052
39. Zhao Q, Feng DC, Hao JC (2011) J Mol Model 17:2817–2823
40. Li QZ, Li R, Liu XF, Li WZ, Chen JB (2012) Chem Phys Chem 13: 1205–1212
41. Li R, Li QZ, Chen JB, Liu ZB, Li WZ (2011) Chem Phys Chem 11: 2289–2295
42. Lu YX, Liu YT, Li HY, Zhu X, Liu HL, Zhu WL (2012) J Phys Chem A 116:2591–2597
43. Li HY, Lu YX, Liu YT, Zhu X, Liu HL, Zhu WL (2012) Phys Chem Chem Phys 14:9948–9955
44. Manna D, Mugesh G (2012) J Am Chem Soc 134:4269–4279
45. Metrangolo P, Resnati G (2012) Nat Chem 4:437–438
46. Boys SF, Bernardi F (1970) Mol Phys 19:553–566
47. Frisch MJ (2009) Gaussian 09 (Revision B.01). Gaussian Inc, Pittsburgh
48. Lu T, Chen FW (2012) J Comp Chem 33:580–592
49. Reed AE, Curtiss LA, Weinhold F (1998) Chem Rev 88:899–926
50. Bader RFW (1990) Atoms in molecules. A quantum theory. Oxford University Press, New York
51. Todd A Keith (2013) AIM All Version 13.05.06, aim.tkgristmill.com